



HAL
open science

Experimental and theoretical confirmation of the role of higher order mechanisms in the electron impact double ionization of helium

E M Staicu Casagrande, C Li, A Lahmam-Bennani, C Dal Cappello, M Schulz, M Ciappina

► To cite this version:

E M Staicu Casagrande, C Li, A Lahmam-Bennani, C Dal Cappello, M Schulz, et al.. Experimental and theoretical confirmation of the role of higher order mechanisms in the electron impact double ionization of helium. *Journal of Physics B: Atomic, Molecular and Optical Physics*, 2011, 44 (5), pp.55201. 10.1088/0953-4075/44/5/055201 . hal-00600136

HAL Id: hal-00600136

<https://hal.science/hal-00600136>

Submitted on 14 Jun 2011

HAL is a multi-disciplinary open access archive for the deposit and dissemination of scientific research documents, whether they are published or not. The documents may come from teaching and research institutions in France or abroad, or from public or private research centers.

L'archive ouverte pluridisciplinaire **HAL**, est destinée au dépôt et à la diffusion de documents scientifiques de niveau recherche, publiés ou non, émanant des établissements d'enseignement et de recherche français ou étrangers, des laboratoires publics ou privés.

Experimental and theoretical confirmation of the role of higher order mechanisms in the electron impact double ionisation of Helium

E M Staicu Casagrande^{1,2}, C Li^{1,2}, A Lahmam-Bennani^{1,2,§}, C Dal Cappello³, M Schulz⁴ and M Ciappina^{5,6}

¹ Université Paris-Sud 11, Institut des Sciences Moléculaires d'Orsay (ISMO, UMR 8214), Bât. 351, 91405 Orsay Cedex, France

² CNRS-ISMO, Bât. 351, 91405 Orsay Cedex, France

³ Université Paul Verlaine-Metz, Laboratoire de Physique Moléculaire et des Collisions, ICPMB (FR 2843), Institut de Physique, 1 rue Arago, 57078 Metz Cedex 3, France

⁴ Dept. of Physics and LAMOR, Missouri University of Science & Technology, Rolla, MO 65409

⁵ Institute of High Performance Computing, 1 Fusionopolis Way, 16-16 Connexis, 138632 Singapore

⁶ Present address: ICFO-Institut de Ciències Fotòniques, 08860 Castelldefels (Barcelona), Spain

§ author to whom all correspondence should be addressed
e-mail : azzedine.bennani@u-psud.fr

PACS 34.80.Dp (also 34.50.Fa and 34.80.-I, and 34.10.+x)

Abstract

Our recent measurements [Lahmam-Bennani *et al* 2010 *J. Phys. B: At. Mol. Opt. Phys.* **43** 105201] of the (e,3-1e) four-fold differential cross sections (4DCS) for double ionisation of helium are here extended to a wider range of ejected electron energies and very asymmetric energy sharing. The previous observations of large angular shifts in the experimental 4DCS distributions with respect to the momentum transfer axis are once again reproduced by the new measured data. Moreover, comparison of all the data sets with the kinematical analysis previously given and with two newly developed non-first order theoretical models for double ionisation, namely ‘the two-step2 – Monte Carlo Event Generator (TS2-MCEG) and a second Born approximation (B2) confirms our interpretation which allows relating the observed shifts and the existence of structures in the intensity distributions mostly to the second order, ‘two-step 2’ (TS2) double ionisation mechanism, which is shown to predominate over the first-order ‘shake-off’ (SO) and ‘two-step 1’ (TS1) mechanisms under the present kinematics.

1. Introduction

The study of double and multiple ionisation processes by charged particle impact has received a considerable interest in the last decade or so, with a strong focus being put on getting a close insight of the role and of the relative importance of the various mechanisms responsible for double ionisation (DI) processes. The progress in computational methods, together with the spectacular development of multi-parameter detection techniques, opened up the way to performing complete experiments in which all kinematical parameters (vector momenta and energies) of all involved particles are determined. Electron impact (e,3e) experiments for DI are one of the most fundamental of such processes, though they remain difficult to perform because they necessitate the *triple coincidence* detection of three particles in the final state (three electrons [1,2] or alternatively the residual ion plus two electrons [3]). To circumvent this difficulty, Lahmam-Bennani and coworkers developed, in a series of papers [4-11], (e,3-1e) experiments where, with respect to the (e,3e) case, one electron is not detected, hence only necessitating a *double coincidence* experiment similar to an (e,2e) single ionisation (SI) but with energetics corresponding to DI. In all these works as well as in further works by other groups [12-15], it was clearly demonstrated that (e,3-1e) experiments provide a very sensitive mean to identify the role of various mechanisms responsible for electron impact DI and to gauge their relative importance.

In a recent study [16] we reported the measurement of the (e,3-1e) four-fold differential cross sections (4DCS) for DI of helium in coplanar asymmetric geometry for a large range of ejected electron energies and at an incident energy of about 600 eV. The experimental angular distributions of the 4DCS displayed large angular shifts of the forward and backward lobes with respect to the momentum transfer direction or its opposite, respectively, as well as a breaking of symmetry with respect to these directions. These observations are clear signatures of the presence of non-first order mechanisms in the DI process. [We briefly recall (see e.g. [16-18]) that first order or first Born mechanisms (in the Born series) involve only one single interaction of the projectile with the target. This is the case for the so-called ‘shake-off’ (SO) and ‘two-step 1’ (TS1) mechanisms. Whereas second order or second Born mechanisms such as ‘two-step 2’ (TS2) involve two successive projectile - target interactions]. A qualitative, kinematical analysis was given in [16] which allowed relating these shifts and the observed structures in the intensity distributions to the second order, ‘two-step 2’ DI mechanism, which was shown to predominate over the first-order ‘shake-off’ and ‘two-step 1’ mechanisms under the investigated kinematics. Such conclusion strongly supports those previously drawn from

(e,3-1e) experiments by Lahmam-Bennani *et al* [11] or from full (e,3e) experiments by Lahmam-Bennani *et al* [19] and by Dorn *et al* [20] and also from the theoretical analyses given in [19] and more recently in [21,22].

The aim of the present work is to extend the study in [16] in two directions: (i) first, by producing more experimental data so as to extend the investigated kinematics to larger ejected electron energies and hence larger energy loss suffered by the projectile, in order to validate or invalidate the observations made in [16] and the kinematical analysis therein given; (ii) and second by comparing the experimental results with two different, newly developed non-first order theoretical predictions, based on a second Born treatment on the one side [21] and on a Monte Carlo approach to TS2, on the other side [22]. (In the absence at the time of elaborate non-first order calculations, the experimental data in [16] were only compared to first order theoretical results.) Our objective is to add further evidence from both experiment and theory that at the impact energy of the present work ($\sim 600\text{-}700$ eV) DI of Helium atom is dominated by non-first order mechanisms such as TS2.

2. Experiment

The experimental set-up and experimental procedure used in the present work are described in detail in [23]. The main characteristic of the spectrometer is the unique combination of three high-efficiency, multi angle toroidal electrostatic energy analysers. Briefly, a monochromatic electron beam with energy $E_0 \sim 600 - 700$ eV (see below) impinges on the gas jet formed at the collision centre. A coplanar geometry is used, where all electrons are observed in the collision plane defined by the incident and scattered momentum vectors, \mathbf{k}_0 and \mathbf{k}_a , respectively. The fast, forward-scattered electron (indexed ‘a’) is detected at the scattered energy $E_a = 500$ eV and at two symmetrical scattering angles, $\theta_a = + (6^\circ \pm 3^\circ)$ and $-(6^\circ \pm 3^\circ)$ as set by input slits at the entrance to the electrostatic lenses associated with the ‘a’-toroidal analyser. Throughout this work, positive angles are counted clockwise starting from the incident electron beam direction. Among the two ejected electrons resulting from DI of the target, (labelled ‘b’ for the faster and ‘c’ for the slower), we choose to detect only the faster one, with energy E_b , in coincidence with the ‘a’-scattered electron, hence an (e,3-1e) experiment. Of course, such distinction does not hold for the equal energy sharing condition, but the same labelling ‘b’ is kept for the detected electron. These ‘b’-electrons are multi-angle analysed in a double toroidal analyser over the angular ranges $\theta_b = 20^\circ - 160^\circ$ and $200^\circ -$

340°, where 0° is defined by the incident beam direction. In the off-line analysis, the total θ_b - angular range is divided into sectors of width $\Delta\theta_b = 5^\circ$. Though the emission direction of the third, ‘c’-electron is unknown, its kinetic energy E_c is known from the energy conservation $E_0 - IP^{2+} = E_a + E_b + E_c$, where IP^{2+} is the He DI potential. [Here, the translational energy of the target atom and the recoil energy transferred to the ion after the emission of the two electrons are neglected, due to the small electron to ion mass ratio]. The experiments were performed at a variety of ejected electron energies ranging from 5 to 144 eV and corresponding either to an equal ($E_b = E_c$) or an unequal ($E_b > E_c$) energy sharing among electrons ‘b’ and ‘c’. We also note the very large range of energy loss ($E_0 - E_a$) suffered by the projectile, from 101 to 235 eV. The incident energy (E_0) is consequently adjusted to fulfil the energy conservation requirement for the Helium target under study, with $IP^{2+} = 79$ eV. The investigated kinematical conditions are summarized in Table 1 where for completeness we also include the data sets published in [16] as they are also used in the discussion given in the present paper.

Case	$E_a = 500$ eV			$\theta_a = -6$ deg		
	E_0 (eV)	E_b (eV) detected	E_c (eV) undetected	K (au)	θ_K / θ_{-K} (deg)	$\theta_{F-TS2} / \theta_{B-TS2}$ (deg)
(a)*	601	17	5	0.88	46 / 226	82 / 290
(b)*	621	37	5	0.96	41 / 221	79 / 297
(c)*	658	74	5	1.12	34 / 214	74 / 307
(d)	663	72	12	1.14	34 / 214	76 / 300
(e)	735	144	12	1.46	26 / 206	67 / 315
(f)*	613	17	17	0.93	43 / 223	84 / 282

*Table 1. Kinematical parameters (energies and momenta) used in this study. Experimental data for the cases indicated with the superscript * have been published in [16]. The last column indicates the directions of ejection of the ‘b’-electron in the forward and backward directions (θ_{F-TS2} and θ_{B-TS2} , respectively) as predicted by the given kinematical analysis, see text.*

Given the above experimental parameters, the momentum transfer to the target, defined by $\mathbf{K} = \mathbf{k}_0 - \mathbf{k}_a$, varies in magnitude from $K = 0.88$ au at $E_b + E_c = 22$ eV (case (a) of Table 1) to $K = 1.46$ au at $E_b + E_c = 156$ eV (case (e)), while its direction θ_K (shown in the 6th column of Table 1) varies from $\sim 46^\circ$ to $\sim 26^\circ$ for these two extreme cases. Simultaneously, due to the

quite large acceptance in θ_a -angle, $\Delta\theta_a = \pm 3^\circ$, the momentum transfer resolution amounts to $\Delta K \sim \pm 0.2$ au and the uncertainty in the momentum transfer direction is $\Delta\theta_K \sim \pm 10^\circ$.

3. Results and discussion

The angular distributions of the (e,3-1e) four-fold differential cross sections (4DCS), $d^4\sigma/dE_a dE_b d\Omega_a d\Omega_b$, for DI of He are shown in figure 1(a) to 1(f) at the various energy sharings listed in Table 1. The experimental results in Fig. 1(a) to (c) and in 1(f) have been previously published in [16]. They are reproduced here for the completeness of the discussion. The other cases are unpublished, new results.

The data are first compared with the calculated results obtained using the first Born BBK or 3C model where the final state, orthogonalized to the initial state, is described by the product of three Coulomb waves [24,25]. Two of these Coulomb functions describe each electron in the field of the target nucleus and the third function describes one electron in the field of the second electron, i.e. takes into account the electron-electron correlation in the continuum. The initial state is described by a wave function which only includes a part of the radial correlation [21]. These calculations, which are shown as dotted curves in Fig. 1, only include first-order DI mechanisms, namely the SO and TS1. Note that the experiments are obtained on a relative scale and have been normalized to the calculations at the maximum of the forward lobe. Here, the labels forward lobe and backward lobe designate the lobe pointing roughly in the momentum transfer direction ($+\mathbf{K}$) and in the opposite direction ($-\mathbf{K}$), respectively. These two directions are indicated by the vertical dotted lines in the figures. A pronounced disagreement is found between this first-order theory and experiments. For all energy sharings considered in figure 1, the most remarkable differences are:

(i) the breaking of symmetry about $\pm\mathbf{K}$ directions in the measured distributions whereas the calculated ones do show such symmetry,

(ii) the large shift in the angular position of the experimental lobes, $\sim 30^\circ$ to 70° with respect to $\theta_{\pm K}$. The uncertainty in the momentum transfer direction due to the angular resolution in θ_a is $\sim 10^\circ$, that is significantly smaller than the observed shift, and hence it only marginally affects this shift.

(iii) the existence of structures in these lobes.

These features are clear evidence that strong non-first Born effects are present in the (e,3-1e) 4DCS distributions, that is, the contribution of the TS2 mechanism to the DI process is

sufficiently important with respect to that of SO and/or TS1 to impose its finger print on the angular distributions. We thus confirm the observations made in [16] and earlier in [11].

As a second facet of this discussion, we now apply the kinematical analysis proposed in [16] which is meant to give a qualitative interpretation of the observed structures as well as an estimate of the angular positions of the lobes in terms of the physical effects due to the TS2 mechanism. This analysis is described in details in [16], hence it will only briefly be summarized here. TS2 is a two-step process: in the first step, the slowest ‘c’-electron is ejected in an (e,2e) ionising process of the He atom, where the corresponding scattered electron (called ‘a*’) appears with the highest probability at the Compton scattering angle, $\pm\theta_{a^*}$, corresponding to the Bethe ridge [26,27]. The \pm sign stands for the fact that the intermediate ‘a*’-electron may appear on both sides of the incident beam direction. In the second step of TS2, the ‘a*’-electron plays the role of the incident projectile in a new (e,2e) ionisation of the intermediate He^+ ion, resulting in the pair (‘a’:‘b’) of electrons effectively detected, where the ‘a’-scattered one is observed with $E_a = 500$ eV under $\theta_a = -6^\circ$, whereas the ‘b’-ejected one appears mostly along the corresponding momentum transfer direction of this new collision, noted here θ_{TS2} . To define this direction, one has to consider two scenarios, depending whether the intermediate ‘a*’-electron is scattered at $+\theta_{a^*}$ or $-\theta_{a^*}$. Each of these scenarios yields an ejected ‘b’-electron either in the forward direction or in the backward direction, noted θ_{F-TS2} and θ_{B-TS2} , respectively. The so predicted θ_{F-TS2} and θ_{B-TS2} values are listed in the last column of Table 1 for each of the kinematics considered here. They are also indicated in Fig. 1 by the vertical dashed lines. Remarkably, all the experimental data shown in Fig. 1 do display prominent structures (for both the forward and the backward distributions). The angular positions of the structures located at the largest angles very nicely agree with the predicted θ_{F-TS2} and θ_{B-TS2} values. This holds for all energy sharings considered in this work, from the equal (case (f)) to the highly unequal (case (e)) sharing. We thus conclude that the forward and backward lobes positions in Fig. 1 are essentially determined by the TS2 contribution, according to the above qualitative kinematical analysis where the TS2 process is considered as two successive, independent (e,2e) single ionisation of the target. First-order SO and TS1 contributions are also present as seen by the significant intensity near the momentum transfer direction, θ_K , and its opposite, θ_{-K} . In some cases, even separate maxima at θ_K are observed. Nevertheless, there the intensity appears to be appreciably smaller than that of the TS2, more so for the backward lobe.

In the third facet of this discussion we compare our measured 4DCS distributions with the calculated results obtained using two newly developed theoretical models. The first model is based on the first Born approximation (FBA), but higher order effects are incorporated using the Monte Carlo Event Generator (MCEG) technique. This approach was successfully applied first to DI by ion impact [28] and more recently extended to electron impact [22]. The method makes use of the MCEG technique to simulate the TS2 mechanism by convoluting two SI events which are both calculated in the FBA. These are successively the SI of the He atom by the incident electron and that of the resulting He⁺ ion by the intermediate scattered electron. In the following, this model is termed TS2-MCEG. Note that the basic idea of this two steps ‘decomposition’ is the same here as that of the kinematical model considered above.

The second theoretical model is more elaborate as it makes use of the second Born approximation and the closure approximation in the way described in [21]. In this model (termed here B2) the final state is described by the approximate BBK wave function, since the use of the full 3C wave-function with the second Born approximation needs much computer time especially for (e,3-1e). The initial state is again described by a wave function which only includes a part of the radial correlation [21] and the final state is orthogonalized to the initial one. The well-known closure approximation [29] is used with a parameter corresponding to the average excitation energy fixed here to 79 eV. This value corresponds to the energy of the initial state.

The results obtained within these two models, TS2-MCEG and B2, are also displayed in Fig. 1. The main general observation is the overall improved agreement with experiments, as compared to FBA-3C results discussed above. Indeed, although both theories do yield some differences in their results, in particular for electron emission in the backward direction, they both succeed in producing forward and backward lobes which now are shifted with respect to $\pm \mathbf{K}$ directions and also have additional structures, especially in the backward region, similar to the behaviour found in the experimental data. In particular, the measured positions of the structures located at angles larger than θ_{+K} and θ_{-K} , respectively, are at least qualitatively (if not quantitatively) predicted by both non-first order models, may be save the equal energy sharing case in Fig. 1(f) where the agreement between second-order theories and experiments is somewhat less satisfactory. Remarkably, these predicted positions are in quite good agreement with the θ_{F-TS2} and θ_{B-TS2} values listed in Table 1 and derived from our very simple kinematical model discussed above. These observations, together with the construction of the TS2 description (based on two successive SI (e,2e) events) as done both in the kinematical model and in TS2-MCEG model, leads us to the conclusion that the lobes located at the

largest angles can be attributed to the TS2 contribution, whereas the ones located at smallest angles are grossly peaking at $+\mathbf{K}$ or $-\mathbf{K}$ direction, and hence may be attributed to the first-order SO and/or TS1 contributions. This conclusion appears to be valid for all cases considered here, independently of the energy sharing among the two ejected electrons.

We also note two further observations:

- at least for the backward lobes, the relative contribution to the measured as well as the calculated 4DCS of the second-order contribution (located at about θ_{B-TS2}) is generally larger than that of the first-order contribution at about θ_K meaning that “non-first order mechanisms such as TS2” dominates over the first-order ones, SO and TS1.
- Apart from the structures we discussed up to now, additional structures in the measured intensity distributions of Fig. 1 seem to be present. Two causes for these structures are conceivable: other non-first order mechanisms, and/or interference effects. (i) A possible candidate for non-first order mechanisms other than TS2 which have not been considered here was recently invoked by Schulz *et al* [30] in the context of fast p + He collisions, where it is the dominant double ionisation process. The authors labelled it Two-Step 1–Elastic mechanism (TS1-EI). It can be viewed as follows: first, a TS1 process leads to the ejection of both target electrons, and then the projectile is elastically scattered from one of the two continuum electrons (hence the alternative label ‘3steps – 2 interactions’ 3S2). As in TS2, the symmetry about \mathbf{K} direction is broken because of this double interaction of the projectile with the target. However, the kinematical analysis presented in this work as well as the model calculations within TS2-MCEG and B2 frameworks cannot be straightforwardly applied to this mechanism. (ii) the observed additional structures might also be due to interferences between all these various competing processes which all lead to the same final state. With a detailed theoretical description missing, the discussion of these interference effects is difficult.

4. Conclusion

We have extended our previous (e,3-1e) experiments for double ionisation of He at ~ 600 - 700 eV impact energy to larger ejected energies and more asymmetric energy-sharing. Our new data also display large shifts as well as marked structures in the forward and backward lobes for the ejected electron angular distributions, similar to the observations made in [16]. For all data sets, our previous qualitative analysis based on kinematical arguments shows that

under the present kinematics the two-step 2 (TS2) mechanism dominates over the SO and the TS1 and is mostly responsible for the structures and angular positions of the measured lobes.

The first Born-3C prediction does not reproduce the observed shifts and structures of the cross section distribution, whereas the theoretical results from two newly developed models, namely the TS2-MCEG and B2 treatments, very clearly constitute a considerable improvement, both for the position of the forward lobe which is correctly reproduced and for the structure of the backward lobe which is qualitatively well predicted. This confirms again that under the present kinematics the non-first order mechanisms such as TS2 are mostly responsible for the structures observed in the measured distributions. Other mechanisms such as TS1-EI may also contribute, but the present models cannot be straightforwardly applied to these mechanisms.

Acknowledgment

We wish to acknowledge Tom Kirchner for his significant involvement in the development of the MCEG based calculations. C Li acknowledges a PhD grant from the China Scholarship Council.

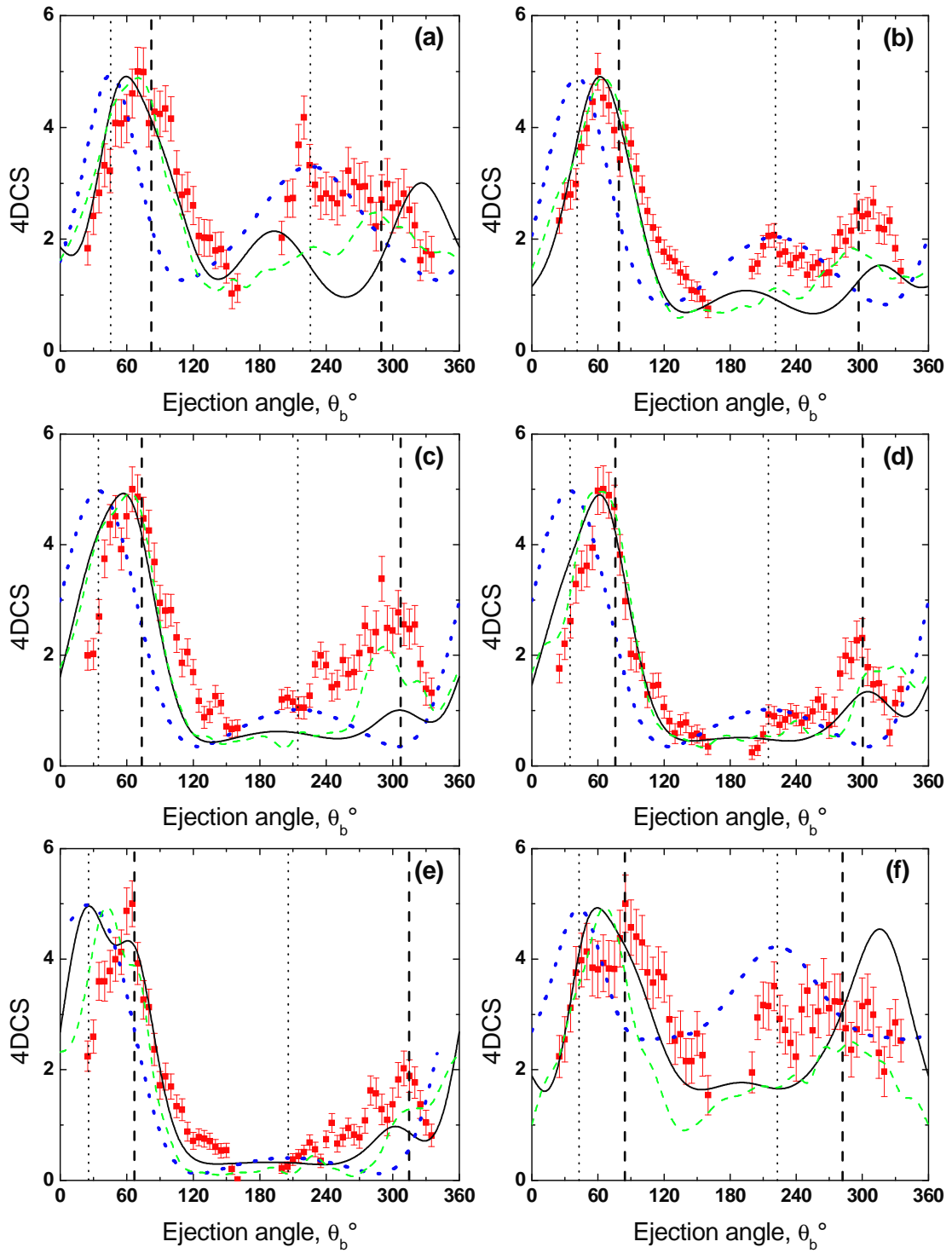
Caption to figure

Figure 1 (Color online): Four-fold differential cross sections (4DCS) for double ionisation of He. The scattered electron with energy $E_a = 500$ eV is detected at an angle $\theta_a = -6^\circ$ in coincidence with the fast-emitted electron with energy E_b , whereas the slow-emitted electron with energy E_c remains undetected. Panel (a): $(E_b : E_c) = (17 : 5)$ eV, (b): $(E_b : E_c) = (37 : 5)$ eV, (c) $(E_b : E_c) = (74 : 5)$ eV, (d): $(E_b : E_c) = (72 : 12)$ eV, (e): $(E_b : E_c) = (144 : 12)$ eV and (f): $(E_b : E_c) = (17 : 17)$ eV. Full squares are the experimental data, with one standard deviation statistical error bar. Theoretical models' predictions are from: first-order FBA-3C (dotted blue curves), TS2-MCEG (dashed green curves) and second-order B2 (full black curves). The 4DCS scale shown is arbitrary, where all experimental and theoretical results are inter-normalised for best visual fit at the maximum of the forward lobe. The thin dotted vertical lines indicate the direction of the momentum transfer (θ_K) and its opposite (θ_{-K}). The heavy dashed vertical lines indicate the directions of ejection of the 'b'-electron, (θ_{F-TS2} and θ_{B-TS2}) as predicted by the given kinematical analysis, see text.

References

- [1] Lahmam-Bennani A, Dupré C and Duguet A 1989 *Phys. Rev. Lett.* **63** 1582
- [2] Taouil I, Lahmam-Bennani A, Duguet A and Avaldi L 1998 *Phys. Rev. Lett.* **81** 4600
- [3] Dorn A, Mosshammer R, Schröter C D, Zouros T J M, Schmitt W, Kollmus H, Mann R and Ullrich J 1999 *Phys. Rev. Lett.* **82** 2496
- [4] Dupré C, Lahmam-Bennani A and Duguet A 1991 *Meas. Sci. Technol.* **2** 327
- [5] Duguet A, Dupré C and Lahmam-Bennani A 1991 *J. Phys. B: At. Mol. Opt. Phys.* **24** 675
- [6] Lahmam-Bennani A, Ehrhardt H, Dupré C and Duguet A 1991 *J. Phys. B: At. Mol. Opt. Phys.* **24** 3645
- [7] Duguet A and Lahmam-Bennani A 1992 *Z Phys D: At., Mol. Clusters* **23** 383
- [8] El Marji B, Duguet A, Lahmam-Bennani A, Lecas M and Wellenstein H F 1995 *J. Phys. B: At. Mol. Opt. Phys.* **28** L733
- [9] El Marji, Lahmam-Bennani A, Duguet A and Reddish T J 1996 *J. Phys. B: At. Mol. Opt. Phys.* **29** L157
- [10] El Mkhater R, Dal Cappello C, Lahmam-Bennani A and Popov Yu V 1996 *J. Phys. B: At. Mol. Opt. Phys.* **29** 1101
- [11] Lahmam-Bennani A, Duguet A and Roussin S 2002 *J. Phys. B: At. Mol. Opt. Phys.* **35** L59
- [12] Ford M J, El Marji B, Doering J P, Moore J H, Coplan M A and Cooper J W 1998 *Phys. Rev. A* **57** 325
- [13] Kouzakov K A and Popov Yu V 2002 *J. Phys. B: At. Mol. Opt. Phys.* **35** L537
- [14] Bolognesi P, Jia C C, Avaldi L, Lahmam-Bennani A, Kouzakov K A and Popov Yu V 2003 *Phys. Rev. A* **67** 034701
- [15] Watanabe N, Khajuria Y, Takahashi M, Udagawa Y, Vinitsky P S, Popov Yu V, Chuluunbaatar O and Kouzakov K A 2005 *Phys. Rev. A* **72** 032705
- [16] Lahmam-Bennani A, Staicu Casagrande E M, Naja A, Dal Cappello C and Bolognesi P 2010 *J. Phys. B: At. Mol. Opt. Phys.* **43** 105201
- [17] Carlson T A and Krause M O 1965 *Phys Rev* **140** 1057
- [18] McGuire J H 1982 *Phys. Rev. Lett.* **49** 1153
- [19] Lahmam-Bennani A, Duguet A, Dal Cappello C, Nebdi H and Piraux B 2003 *Phys. Rev. A* **67** 010701(R)
- [20] Dorn A, Kheifets A, Schröter C D, Höhr C, Sakhelashvili G, Mosshammer R, Lower J and Ullrich J 2003 *Phys. Rev. A* **68** 012715; see also ‘Comment’ by Lahmam-Bennani A, Catoire F, Duguet A and Dal Cappello C 2005 *Phys. Rev. A* **71** 026701; and ‘Reply to Comment’ by Dorn A *et al* 2005 *Phys. Rev. A* **71** 026702
- [21] Dal Cappello C, Haddadou A, Menas F and Roy A C 2011 *J. Phys. B: At. Mol. Opt. Phys.* **44** 015204
- [22] Ciappina M F, Schulz M and Kirchner T 2010 *Phys. Rev. A* **82** 062701
- [23] Catoire F, Staicu Casagrande E M, Lahmam-Bennani A, Duguet A, Naja A, Ren X G, Lohmann B and Avaldi L 2007 *Rev. Sci. Instrum.* **78** 013108
- [24] Joulakian B, Dal Cappello C and Brauner M 1992 *J. Phys. B: At. Mol. Opt. Phys.* **25** 2863
- [25] Ancarani L U, Gasaneo G, Colavecchia F D and Dal Cappello C 2008 *Phys. Rev. A* **77** 062712
- [26] Lahmam-Bennani A, Wellenstein H F, Dal Cappello C, Duguet A and Rouault M 1983 *J. Phys. B* **16**, 2219
- [27] Avaldi L, Camilloni R, Fainelli E, Stefani G, Franz A, Klar H and McCarthy I E 1987 *J. Phys. B: At. Mol. Phys.* **20** 5827

- [28] Fischer D, Schulz M, Schneider K, Ciappina M, Kirchner T, Kelkar A, Hagman S, Grieser M, Kühnel K -U, Moshhammer R and Ullrich J 2009 *Phys. Rev. A* **80** 062703
- [29] Byron F W Jr, Joachain C J and Piraux B 1980 *J. Phys. B: At. Mol. Phys.* **13** L673
- [30] Schulz M, Ciappina M F, Kirchner T, Fischer D, Moshhammer R and Ullrich J 2009 *Phys. Rev. A* **79**, 042708



Staicu Casagrande E M *et al*

Figure 1